

Quantification and Risk Assessment of PAHs in Street Dust from Functional Areas of Khamis-Mushait, Saudi Arabia

Tarek O. Said^{1*}, Nasser S. Awwad¹, Fatimah A. El Amri², Abubakr M. Idris², and ³Ali Yahya A. Alalmie

¹National Institute of Oceanography and Fisheries (NIOF), Egypt

²Department of Chemistry, College of Science, King Khalid University, Abha, Saudi Arabia

³The Poison Control and Medical Forensic Chemistry Centre, Asir, 6922, Saudi Arabia

*Corresponding author

Tarek O. Said, National Institute of Oceanography and Fisheries (NIOF), Egypt

Submitted: 23 Jul 2022; Accepted: 27 Jul 2022; Published: 01 Aug 2022

Citation: Said TO*, Awwad NS, Amri FA El, Idris AM, and Alalmie AYA. (2022). Quantification and Risk Assessment of Pahs in Street Dust from Functional Areas of Khamis-Mushait, Saudi Arabia. *J Gene Engg Bio Res*, 4(2), 253- 270.

Abstract

The average value of polycyclic aromatic hydrocarbons (PAHs) in Khamis-Mushait street dust was 2809.46 ng/g, ranging from 1250.41-4249.29 ng/g. Incinerator and industrial locations had the highest concentration of fossil PAHs (Σ FPAHs), accounting for 69.62% of PAHs. The highest concentrations of carcinogenic PAHs (Σ CARC) and combustion PAHs (Σ COMB) were found in the King Fahd Garden and Al-Hayat National Hospital regions, accounting for 41.70 % and 27.46 % of PAHs, respectively. Naphthalene (NAP), Acenaphthylene (ACY) and Acenaphthene (ACE) were > effective range low (ERL). However, ACE was > effective range medium (ERM), and ACY, ACE, and DBA (dibenzo anthracene) were > Probable Effect Level (PEL). Furthermore, the effects of NAP, fluoranthene (FLT), pyrene (PYR), and benzo (a)pyren (BaP) were greater than the threshold effect level (TEL). The order of Hazardous indices (HI) for both children and adults were ACE > ACY > NAP > PYR > fluorene (FLR) > FLT > benzo (ghi) perylene (BghiP) > phenanthrene (PHN) > ANT. However, total HI for non-cancer risks for PAHs were 2.69×10^{-2} - 9.91×10^{-5} and 2.50×10^{-2} - 9.22×10^{-4} to adults and children, respectively. These values considered safe level and insignificant to adults and children. In addition, ACE may pose risk based on acute and intermediate oral exposure. The cluster analysis of dust samples declared the following order from different sources: traffic > industrial > commercial.

Keywords: Risk, PAHs, Street Dust, Saudi Arabia

Introduction

Street dust is the result of those emissions depositing on paved streets, which consists of a complex mixture of components including vehicle exhaust, tire and brake pad wear, spillage, and leakage. It is considered as indicator for the quality of urban environment [1]. Dust can easily transport and accumulate many pollutants such as heavy metals and organic compounds [2]. Polycyclic aromatic hydrocarbons (PAHs) have received more attention, as they can combine with solids in large quantities because of their hydrophobic properties [3]. The Stockholm Convention and USEPA have classified 16 PAHs as priority list [4]. Previous studies demonstrated that exposure to PAHs may increase oxidative DNA damage of human body [5]. The potential risks of PAHs exposure in street dust for people who working or living in the roadside area have attracted international attention. Found that the main cause of the carcinogenic risk of PAHs to adults or children was proved

by four-rings PAHs of PYR, BbF and BkF through ingestion and dermal-contact pathways [6, 7]. IARC (International Agency for Research on Cancer) and ATSDR (Agency for toxic substances and diseases registry) has classified PAHs in priority pollutant list due to their mutagenic and carcinogenic properties [8]. A previous study was made through estimation of PAHs in Jeddah, Saudi Arabia. Their results were lower compared to Riyadh, Tehran and Egypt and higher compared to Kuwait, while within the same levels in Damascus [9]. Another study was conducted in Jeddah's schools to evaluate the concentration levels of PAHs (indoor) in air conditioner filter dust of some primary schools in Jeddah city. In all schools DBA, BaP and BbF were the predominant contributors to cancer effect [10, 11]. Recorded PAHs ranged from 90-22146 ng/g with an average of 4096 ng/g in dust from different carpets of mosques in Riyadh city. The result showed that the origins of these contaminations are from petrogenic inputs from traffic,

stack emission and pyrogenic resulting perfumed wood burning application after cleaning of the mosque. Σ 16 PAHs concentrations during winter and summer were varied from 2.15-10.6 with a median value of 4.61 mg/kg in street dust sampled park area, educational area, commercial area residential area, and traffic area of Chengdu, China [12]. They reported also that carcinogenic risk by ILCR (Incremental lifetime cancer risk) model for PAHs in street dust indicates an acceptable potential cancer risk for residents. Consequently, it is necessary to carry out the investigation of the relationship between the concentrations and risks of PAHs in street dust and urban functional area characteristics in the core city of khamees-Mushait. The results will benefit in relation to identify possible sources of PAHs in the area, and to assess their potential health risk.

Materials and Methods

Khamees-Mushait city is located in the southern-western part of Saudi Arabia at 18.18N, 42.44E with a total area of 1,353 km² (Figure 1). The city is located on a flat plain surrounded by high altitude areas. Its climate is cold to moderate over the course of a year with humidity of 43–80% and average annual rainfall of 189.3 mm [13]. It contains various industrial activities such as cement, lubricants, pesticides, dyes, marble, and glass, with several different workshops such as blacksmithing, vehicle maintenance, plumbing and heavy equipment. It also includes many markets and large landfill sites for dumping household waste from homes, restaurants, service centers. Moreover, the city is surrounded by

many farms producing different crops [14]. Ninety street dust samples were collected from 30 different sectors in Abha and Khamees-Mushait cities. Triplicate samples of approximately 300g were taken from each station using a clean shovel and brush. From which the top 3 cm were scooped into pre-cleaned wide-mouth plastic bags and transported to the laboratory and stored at –20°C until analysis. The street dust samples were analyzed for PAHs following well-established USEPA 3550B method. In addition, three street dust samples were collected from Aqbat Hbo (as a control area), to determine the background levels for PAHs. All samples were stored in small self-sealing plastic bags, and then kept dry in a freezer until analysis. Thirty grams were exactly weighted and mixed with 10 g anhydrous Na₂SO₄. The ultrasonic extraction was carried out using 80 ml of Acetone/DCM (1:1) for 25 min at 25°C. Then decant all the extracted volumes (240 ml) into vacuum filtration. The extracted was concentrated to 1ml at 30°C using rotary evaporator. The extracted volume was transferred to the top of glass column (50 ml) prepared by slurry packing 20 ml (10 g) of silica (activated at 185 °C over-night and then deactivated with 12.5 % water, followed by 10 ml (10g) of alumina (90 neutral, 70–230 mesh previously activated at 185°C over-night and deactivated with 12.5 % water) and finally 1g of anhydrous Na₂SO₄. The elution was performed using 40 ml of n-hexane/DCM (3:2). Finally, the eluted samples were evaporated using rotary evaporator to < 5 ml, then add 4 ml ACN, evaporate again to < 2 ml, then transfer the extract to 5 ml vial and complete with ACN.

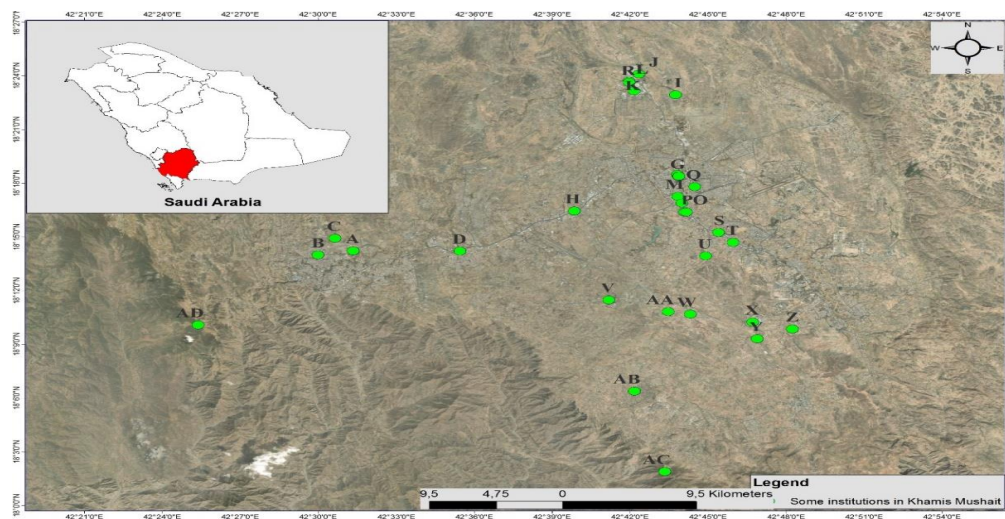


Figure 1: Map of different sectors collected from Khamees-Mushait City, Asir region, KSA.

The extract was filtered using polytetra fluoroethylene (PTFE) syringe filters into 2 ml HPLC vial. Accuracy of tests were performed using spiked samples to verify the recovery (R) as given in equation 1:

$$R = \frac{C_{\text{Experimental}} - C_{\text{Non-spiked}}}{C_{\text{Std}}} \quad (1)$$

$C_{\text{Experimental}}$ is the measured concentration of PAHs in spiked sample. $C_{\text{Non-spiked}}$ is the concentration of PAHs in non-spiked sample. C_{Std} is the concentration of standard solution added to the sample to be spiked. The health risk of exposure to PAHs in the street dust samples to adults and children was assessed [15]. The Chronic daily intake (CDI) values were calculated by equations (2-4):

$$CDI_{\text{Ingestion}} = \left(\frac{C_i \times \text{IngR} \times \text{ExFr} \times \text{ED} \times \text{CF}}{\text{BW} \times \text{AT}} \right) \quad (2)$$

$$CDI_{\text{Inhalation}} = \left(\frac{C_i \times \text{InhR} \times \text{EF} \times \text{ED}}{\text{PEF} \times \text{BW} \times \text{AT}} \right) \quad (3)$$

$$CDI_{\text{dermal}} = \left(\frac{C_i \times \text{SA} \times \text{AF} \times \text{DAF} \times \text{EF} \times \text{ED} \times \text{CF}}{\text{BW} \times \text{AT}} \right) \quad (4)$$

CDI was performed through three major exposure pathways including: ingestion, inhalation, and dermal contact. C_i is the PAH concentration (ng/g) in the dust sample. IngR is the ingestion rate (100 mg/day for adult, 200 mg/day for children). ExFr is the exposure frequency (350 days). ED is the exposure duration (24 years for adult, 6 years for children). BW is the body weight (70 kg for adult, 15 kg for children). AT is the average time (365 x 24 days for adult, 365 x 6 days for children). CF is the conversion factor (1×10^{-6} kg/mg). InhR is the inhalation rate (20 mg/cm² for adult and 7.6 mg/cm² for children). PEF is the particle emission factor (1.36 x 10⁹ m³/kg). SA is the surface area of the skin that contacts the soil (5700 cm²/event for adult and 2800 cm²/event for children).

Table 1: Latitude and Longitude of Different Locations

NO	Sample code	Location	Latitude	Longitude	Activity
1	I a	Abha industrial (1)	N18°14'14"	E42°31'20.6"	Vehicular traffic
2	I b		N18°14'53.5"	E42°30'43.1"	
3	I c		N18°14'55.6"	E42°30'09"	
4	II a	Abha industrial (2)	N18°14'48.5"	E42°30'42.3"	Vehicular traffic
5	II b		N18°14'48.5"	E42°30'33.1"	
6	II c		N18°14'53.2"	E42°30'33.9"	
7	III a	Abha industrial (3)	N18°14'56.1"	E42°30'38.7"	Vehicular traffic
8	III b		N18°14'59"	E42°30'19.5"	
9	III c		N18°14'49.5"	E42°30'40.9"	
10	IV a	Lassan	N18°14'13.2"	E42°35'27.7"	Vehicular traffic
11	IV b		N18°14'09.1"	E42°35'26.2"	
12	IV c		N18°14'09"	E42°35'24"	
13	V a	Gold Market	N18°18'30.2"	E42°43'48.6"	Vehicular traffic and commercial zone
14	V b		N18°18'29.3"	E42°43'45.9"	
15	V c		N18°18'33.1"	E42°43'47.7"	
16	VI a	AL-Hawashi Mosque	N18°18'23.6"	E42°43'51.2"	Vehicular traffic and commercial zone
17	VI b		N18°18'23.3"	E42°43'49.4"	
18	VI c		N18°18'21.7"	E42°43'49"	
19	VII a	Asdaf Mall	N18°18'23.7"	E42°43'52.5"	Vehicular traffic and commercial zone
20	VII b		N18°18'24.5"	E42°43'57.7"	
21	VII c		N18°18'23.4"	E42°43'53.2"	
22	VIII a	Bahes Traffic light	N18°16'27.3"	E42°39'51.1"	Vehicular traffic
23	VIII b		N18°16'25.7"	E42°39'51.7"	
24	VIII c		N18°16'25.4"	E42°39'50.8"	
25	IX a	Incinerator	N18°22'56.5"	E42°43'44.7"	Vehicular traffic

26	IX b		N18°22'53.3"	E42°43'49.9"	
27	IX c		N18°22'49.4"	E42°43'48.1"	
28	X a	Khamees- Mushait industrial (1)	N18°24'06.1"	E42°42'19.6"	Industrial area
29	X b		N18°24'01.9"	E42°42'06.9"	
30	X c		N18°24'01.9"	E42°42'26.8"	
31	XI a	Khamees- Mushait industrial (2)	N18°23'09.9"	E42°42'8.6"	Industrial area
32	XI b		N18°23'19.9"	E42°42'03.3"	
33	XI c		N18°23'15.3"	E42°42'12.5"	
34	XII a	Khamees- Mushait industrial (3)	N18°23'41.8"	E42°41'58"	Industrial area
35	XII b		N18°23'47"	E42°42'18"	
36	XII c		N18°23'38.4"	E42°42'08"	
37	XIII a	Vegetable and date Market area	N18°17'15.8"	E42°43'49.8"	Vehicular traffic and commercial zone
38	XIII b		N18°17'13"	E42°43'39.3"	
39	XIII c		N18°17'12.8"	E42°43'44.3"	
40	XIV a	Abu Dabeel Station	N18°16'54.4"	E42°43'59.6"	Vehicular traffic
41	XIV b		N18°16'54.3"	E42°43'58.5"	
42	XIV c		N18°16'55.7"	E42°43'58.9"	
43	XV a	Khamees- Mushait General Hospital	N18°16'23.9"	E42°44'06.1"	Vehicular traffic
44	XV b		N18°16'29.3"	E42°44'04.8"	
45	XV c		N18°16'23.7"	E42°44'03"	
46	XVI a	Heef Concrete Factory	N18°16'24"	E42°44'09.9"	Concrete factory
47	XVI b		N18°16'24.5"	E42°44'12.1"	
48	XVI c		N18°16'22.7"	E42°44'13.4"	
49	XVII a	King Fahad Garden	N18°17'49"	E42°44'30"	Vehicular traffic
50	XVII b		N18°17'48"	E42°44'22"	
51	XVII c		N18°17'51"	E42°44'28"	
52	XVIII a	Al-Hayat National Hospital	N18°17'26.2"	E42°44'34.6"	Vehicular traffic
53	XVIII b		N18°17'23.7"	E42°44'35.1"	
54	XVIII c		N18°17'23.2"	E42°44'31.9"	
55	XIX a	Al-Beshri Petroleum Station	N18°15'15.7"	E42°45'24.4"	Vehicular traffic
56	XIX b		N18°15'16.6"	E42°45'24.2"	
57	XIX c		N18°15'16.2"	E42°45'25.4"	
58	XX a	Khamees Avenue Mall	N18°14'41.7"	E42°45'57.5"	Vehicular traffic and commercial zone
59	XX b		N18°14'46.5"	E42°45'58.3"	
60	XX c		N18°14'47.5"	E42°45'53.3"	
61	XXI a	Dana Olive Station	N18°13'56.6"	E42°44'54.1"	Vehicular traffic
62	XXI b		N18°13'57.2"	E42°44'52.1"	
63	XXI c		N18°13'55.4"	E42°44'52.7"	
64	XXII a	Sahl Station	N18°11'29.4"	E42°41'10.8"	Vehicular traffic and commercial zone
65	XXII b		N18°11'29.2"	E42°41'07.9"	
66	XXII c		N18°11'27.3"	E42°41'04.3"	
67	XXIII a	Al-Wajih Holding Company	N18°10'41.5"	E42°44'19.3"	Industrial area
68	XXIII b		N18°10'47.2"	E42°44'11.5"	
69	XXIII c		N18°10'53.3"	E42°44'08"	

70	XXIV a	Traffic light in Ahd Rofiadah	N18°10'14.9"	E42°46'43.3"	Industrial area
71	XXIV b		N18°10'16.9"	E42°46'42.7"	
72	XXIV c		N18°10'15.9"	E42°46'43.9"	
73	XXV a	Saif Muhammad Al Ddubsh Factory	N18°09'18.9"	E42°46'53.4"	Concrete factory
74	XXV b		N18°09'21.0"	E42°46'51.8"	
75	XXV c		N18°09'22.9"	E42°46'51.4"	
76	XXVI a	Al- Shuhada Garden	N18°09'51.4"	E42°48'15.2"	Vehicular traffic
77	XXVI b		N18°09'49.5"	E42°48'20.8"	
78	XXVI c		N18°09'47.6"	E42°48'13.5"	
79	XXVII a	Family Medicine Hospital	N18°10'50"	E42°43'28"	Vehicular traffic and commercial zone
80	XXVII b		N18°10'51"	E42°49'35"	
81	XXVII c		N18°10'49"	E42°49'37"	
82	XXVIII a	Dalagan Park	N18°06'23.4"	E42°42'10"	Vehicular traffic
83	XXVIII b		N18°05'46.9"	E42°42'30"	
84	XXVIII c		N18°05'34.1"	E42°42'14.2"	
85	XXIX a	Prince Sultan Park	N18°01'53.6"	E42°43'20"	Vehicular traffic
86	XXIX b		N18°02'31.8"	E42°43'05.9"	
87	XXIX c		N18°03'05.8"	E42°42'54.3"	
88	XXX a	Aqbat Hbo	N18°10'05.5"	E42°25'22.8"	(Control area)
89	XXX b		N18°09'51.8"	E42°25'23.8"	
90	XXX c		N18°10'14.9"	E42°25'00.4"	

AF is the skin adherence factor for soil (0.07 mg/cm for adult, 0.02 mg/cm for children). DAF is the dermal absorption factor (0.001) for all elements [15, 16]. For carcinogens, the lifetime average daily dose ($LADD_{inh}$) through inhalation exposure pathway was calculated for PAHs using equation (5). The carcinogenic risk (CR) was then estimated using equation (6); where CSF is carcinogenic slope factor of PAHs described by Integrated Risk Information System [17, 18].

$$LADD_{inh} = \frac{C \times EF}{PEF \times AT} \times \left(\frac{R_{inhchildren} \times ED_{children}}{BW_{children}} + \frac{R_{inhadults} \times ED_{adults}}{BW_{adults}} \right)$$

$$CR = LADD_{inh} \times CSF$$

HQ is a ratio of the CDI of PAHs through the three pathways. HQ and HI was calculated by equations (7-8)

$$HQ = \frac{CDI}{RFD}$$

$$HI = \sum (HQ_{ingestion} + HQ_{inhalation} + HQ_{dermal})$$

Where RFD is the reference dose, characterizes the health risk of non-carcinogenic adverse effects due to exposure to toxicants. If HI, > 1 indicates possible adverse health effects [19]. The illustrated a set of minimal risk levels (MRLs) for oral exposition of carcinogenic PAHs. The set has been recommended to be used as a

reference for the toxicity evaluation of hazardous substances based on acute (1–14 days) and intermediate (15–365 days) exposition times. The Daily Intake (mg/kg/day) is recommended by as given in equation (9), for comparison with MRLs, where C is the concentration of PAH in $\mu\text{g/g}$ [20].

$$DI = \frac{C \times DC}{BW}$$

To establish inter-PAHs relationships in dust samples, Pearson correlation coefficients (PCC) and cluster analysis (CA) were applied to characterize the sampled sites according to their similarities in term of the contents of five groups of PAHs including 2-rings, 3-rings, 4-rings, 5-rings, and 6-rings. Principal component analysis (PCA) was performed as well to identify sources of 16-PAHs in dust samples. PCA was carried out using the rotation method of Varimax with Kaiser Normalization after extraction. Statistical analyses were carried out by SPSS software version 16.0 for windows.

Results and Discussion

The measurement, reliability, extraction efficiency and accuracy of the results were controlled by spiking analysis with 1000 $\mu\text{g/l}$ of mixed external standard PAHs in the three selected dust samples. The LOD and LOQ were calculated to be ranged from 1.97-94.95 and 6.56-316.50 $\mu\text{g/l}$, respectively for all measured list of standard PAHs and the recovery efficiencies (Table 2).

Table 2: Recovery % for spiked PAHs recorded in three selected dust samples

PAHs	Recovery %			LOD	LOQ
	IX	XI	XXIX		
NAP	43.11	52.161	56.39	2.44	8.12
ACY	57.95	48.44	53.63	18.20	60.68
ACE	51.13	50.21	49.77	7.94	26.48
FLR	69.30	61.98	63.51	88.54	295.15
PHN	74.82	80.44	78.54	1.97	6.56
ANT	71.05	65.11	88.31	13.01	43.38
FLT	75.27	62.19	91.94	58.53	195.09
PYR	89.24	73.39	76.43	7.28	24.28
BaA	88.65	78.99	82.92	7.41	24.68
CHR	75.56	89.67	77.64	10.39	34.64
BbF	78.22	82.33	79.02	19.91	66.36
BkF	80.77	82.11	83.44	7.70	25.68
BAP	81.78	81.23	80.77	6.99	23.29
DBA	89.15	96.82	88.99	37.49	124.98
BghiP	81.22	97.32	98.63	2.16	7.18
IP	79.56	77.55	75.66	94.95	316.50

IX = Incineration area, XI = Khamees-Mushait Industrial area, XXIX = Prince Sultan Park. LOD = limit of detection, LOQ = limit of quantification.

Table 3 and Figures (2-3) indicated that the maximum concentration of Σ FPAHs was recorded at sector IX-XII (Incinerator and Khamees-Mushiat industrial areas) with 2958.23 represent-

ing 69.62% of Σ PAHs. The maximum concentrations of both of Σ CARC and Σ COMB were recorded at sector XVII-XVIII (King Fahd Garden area and Al-Hayat National Hospital area) with 1679.44 and 1106.08 representing 41.70% and 27.46% of Σ PAHs, respectively. It was obvious that the decreasing order of average PAHs categories was Σ FPAHs > Σ CARC > Σ COMB for all sectors.

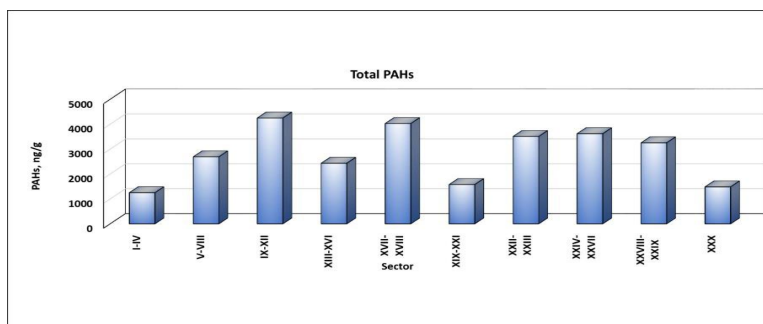


Figure 2: Levels of Σ PAHs concentrations of different sectors.

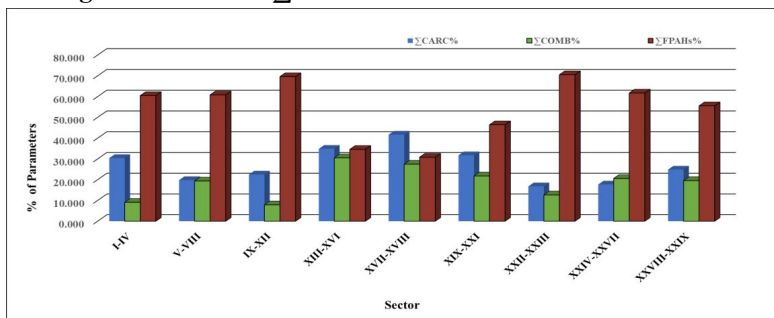


Figure 3: Distribution of the % of Σ CARC, Σ COMB and Σ FPAHs for all sectors

Table 4: declared that the concentrations of NAP, ACY and ACE were > ERL (ERL = 16-160 ng/g); the concentrations of ACE were > ERM (ERM = 500 ng/g); the concentrations of ACY, ACE, DBA were > PEL (PEL = 87-125 ng/g) and the concentrations of NAP, FLT, PYR and BaP were > TEL (TEL = 37-125 ng/g). In addition, similar observations were found relative to the TEL and PEL ac-

ording to [21]. However, the individual PAH concentrations in our study were lower than the national sediment quality criteria for both of ACY and PHN (2400 ng/g), while FLT was exceeded in our investigation with concentrations > 3000 ng/g. Thus, it is obvious that our results may pose a possible health risk to human [22].

Table 3: A comparison between the average residual concentrations (ng/g) of PAHs recorded in all sectors of Abha and Kha-meets-Mushait, Asir region

Compound	Sectors										Av	Min	Max
	I-IV	V-VIII	IX-XII	X I I I - XVI	XVII-XVIII	X I X - XXI	X X I I - XXIII	X X - IV-XX-VII	X X - VIII-XX-IX	XXX			
NAP	68.24	672.46	240.84	169.65	46.20	31.48	215.58	246.87	35.81	15.44	174.26	15.44	672.46
ACY	348.10	107.79	244.53	123.28	165.07	372.49	195.77	202.05	297.51	64.26	212.09	64.26	372.49
ACE	251.95	1091.75	2580.33	420.35	894.77	125.22	2014.76	1559.48	1768.80	1041.70	1174.91	125.22	2580.33
FLR	59.61	3.72	41.16	53.96	112.15	176.25	9.29	131.06	ND	ND	58.72	ND	176.25
PHN	21.87	ND	48.49	52.03	0.05	0.56	38.85	17.54	6.64	ND	18.60	ND	52.03
ANT	6.58	7.58	20.16	22.44	23.89	26.83	0.00	76.55	32.17	ND	21.62	ND	76.55
FLT	30.62	26.34	47.20	19.48	301.78	277.72	63.48	138.87	202.59	8.29	111.64	8.29	301.78
PYR	12.39	110.36	78.05	583.50	257.18	2.86	123.79	271.26	467.07	ND	190.65	ND	583.50
BaA	9.60	18.04	64.00	23.37	123.20	34.35	105.48	73.46	62.01	ND	51.35	ND	123.20
CHR	46.05	0.08	99.55	75.73	141.87	ND	37.70	223.86	ND	ND	69.43	ND	223.86
BBF	24.75	38.97	61.46	198.51	138.50	54.16	14.27	82.47	338.87	ND	95.20	ND	338.87
BKF	3.39	60.33	42.59	0.00	207.90	63.62	154.77	71.46	ND	ND	60.41	ND	207.90
BaP	30.08	71.32	64.98	150.99	248.31	31.02	93.26	91.48	91.76	ND	87.32	ND	248.31
DBA	315.60	330.29	221.73	257.26	29.73	199.39	345.38	28.93	ND	ND	172.83	ND	345.38
BghiP	21.57	49.47	27.28	64.33	197.35	ND	64.69	39.81	ND	354.71	91.02	ND	354.71
IP	ND	103.54	574.47	218.22	1139.71	182.02	31.07	363.54	ND	ND	261.26	ND	1139.71
Total PAHs	1250.41	2692.04	4249.29	2433.10	4027.65	1577.96	3508.14	3618.68	3252.98	1484.41	2809.46	1250.41	4249.29
ΣCARC	380.04	562.16	955.43	848.36	1679.44	500.94	589.46	639.88	808.72	ND	696.44	ND	1679.44
ΣCARC%	30.39	19.80	22.49	34.87	41.70	31.75	16.80	17.68	24.86	ND	24.03	ND	41.70
ΣCOMB	114.03	246.58	335.63	743.03	1106.08	344.20	444.44	745.25	636.71	363.00	507.90	114.03	1106.08
ΣCOMB%	9.12	19.36	7.90	30.54	27.46	21.81	12.67	20.60	19.57	24.45	19.35	7.90	30.54
ΣFPAHs	756.34	1883.30	2958.23	841.71	1242.13	732.82	2474.23	2233.55	1807.54	1121.41	1605.13	732.82	2958.23
ΣFPAHs%	60.49	60.84	69.62	34.59	30.84	46.44	70.53	61.72	55.57	75.55	56.62	30.84	75.55

NAP: naphthalene, ACY: acenaphthylene, ACE: acenaphthene, FLR: fluorene, PHN: phenanthrene, Ant: anthracene, FLT: fluoranthene, PYR: pyrene, BaA: benzo(a)anthracene, CHR: chrysene, BBF: benzo(B)fluoranthene, BKF: benzo(k)fluoranthene, DBA: dibenzoanthracene, BghiP: benzo(ghi)perylene, IP: indenopy-

rene, FPAHs (components of molecular weight < 178 including (ΣNAP, ACY, ACE, FLR, ANT and PHN); ΣCARC (ΣBaA+ BbF+ BaP+DBA+IP) and ΣCOMB (components of molecular weight > 178 including (ΣFLT+PYR+CHR+BkF+BghiP).

Table 4: Comparison between average concentrations of PAHs recorded in Abha and Khamees-Mushait dust with that recorded for the permissible levels

Compound	aERL	bERM	cPEL	dTEL	AV
NAP	160	2100	400	37.5	174.26
ACY	44	640	125	NR	212.09
ACE	16	500	87.5	NR	1174.91
PHN	240	1500	500	75	18.60
ANT	85.3	1100	250	50	21.62
FLT	600	5100	125	12.5	111.64
PYR	665	2600	1400	125	190.65
BaA	261	1600	662	75	51.35
CHR	384	2800	825	100	69.43
BaP	430	1600	750	87	87.32
DBA	63.4	260	125	NR	172.83
Total PAHs	2967	20340	NR	NR	2809.46

^{a,b} cited from, ^{c,d} cited from CCME (2001), ERL = Effects Range-Low, ERM = Effects Range-Median, TEL = threshold effect level, PEL = Probable Effect Level, NR = not recorded in the cited references, Av = average [23].

ANT/(ANT+PHN), FLR/(FLR+PYR), BaA/(BaA+CHR), IP/(IP+BghiP), PHN/ANT, FLT/PYR, LMW-PAHs/HMW-PAHs, PHN/ANT and FLT/PYR are used for the source elucidation. Table 5 declared that PHN/ANT was < 10 indicated pyrolytic source, in addition FLT/PYR ratio was >1.0 in sectors: I-IV, XVII-XVIII and XIX-XXI indicated pyrolytic source. While this ratio was <1.0 in the rest of sectors reflecting petrogenic sources. This finding declared that both of pyrolytic and petrogenic sources as main sources for PAHs in recent study. BaA/CHR ratio was 0.21-229.94, similar to coal and coke emission source (1.05–1.17), mentioned by. BaP/BghiP was ranged from 1.26-2.38 reflecting traffic emissions as the most possible source. BaP/BghiP was > 0.60 often refer to the presence of traffic emissions as mentioned by. In addition, IP/BghiP was > 0.4 reflecting diesel engine source. This is in accordance with who stated that for gasoline engines, IP/BghiP ratio is around 0.40 and reaches 1.00 for diesel engines. ANT/(ANT+PHN) was > 0.1 usually is taken as a dominance source of combustion. FLR/FLR+PYR was < 0.5 suggesting gasoline emissions at all sectors except sectors I-IV and XIX-XXI with ratio > 0.5 indicating diesel emission. FLT/(FLT+PYR) ranged from 0.03 to 1.0 indicating inputs from petroleum and/or liquid fossil fuel combustion source, kerosene, grass, coal and wood combustion as well. Stated that FLT/(FLT+PYR) of 0.5 is usually defined as the petroleum/combustion transition point. FLT/(FLT+PYR) is < 0.4 for most petroleum samples, between 0.4 and 0.5 for of liquid fossil fuel (vehicle and crude oil) combustion and above 0.5 in ker-

osene, grass, most coal and wood combustion. IP/(IP+BghiP) varied between 0.32 - 0.96 indicating inputs from liquid fossil fuels and/or sources of vehicular combustion, as well as those from the process of combustion of biomass and coal as described by . IP/(IP+BghiP) > 0.5 refer to coal combustion, while of 0.62 indicates wood combustion reflecting the same sources for pollution as stated by. LMW/HMW PAHs ratio > 1 refer petrogenic source, while the ratio < 1 in most sectors except XIII-XVI and XVII-XVIII indicate to pyrolytic sources. LMW-PAH/HMW-PAH ratio was > 1, indicate petrogenic source was <1 refer to pyrolytic source. Figure (4) proved that a good correlation was recorded between BbF/BaP and BkF/BaP with $r = 0.399$, suggesting pyrolytic origin of PAHs, this is in accordance with [24-31]. On the other hand, the average concentration of PAHs compounds based on aromatic ring numbers were shown in Table 5 and Figure 5. The descending order for ring structures of PAHs were 3-ring > 5-ring > 4-ring > 6-ring > 2-ring PAHs with average concentrations 1485.934, 461.95, 416.116, 381.309 and 174.258, respectively. The risk from exposure to street dust in term PAHs was assessed; the approaches considered were LADD, CDI, HQ, HI, CR and DI. The health risk to adults and children of the examined PAHs in street dust from the area of study are shown in Table (6) for non-carcinogenic risk, the ingestion of dust particles appeared to be the major route of exposure pathway for PAHs to children and adults, followed by dermal contact and inhalation. The HI values for both children and adults were ACE > ACY > NAP > PYR > FLR > FLT > BghiP > PHN > ANT. HI values of non-cancer risks of all PAHs due to dust exposure were 2.69×10^{-2} – 9.91×10^{-5} and 2.50×10^{-2} – 9.22×10^{-4} to adults and children, respectively. These values are within the safe level and hence it could be concluded that the examined PAHs in dust had insignificant non-cancer risks to adults and children. The carcinogen risks from inhalation exposure of PAHs were 1.41×10^{-10} – 3.67×10^{-7} and 5.66×10^{-10} – 1.47×10^{-6} for adults and children, respectively. The result of DI values and guideline level are presented in Table 7. The results showed that the CR of all PAHs were generally within the acceptable level of 1×10^{-6} (Table 8). The residual levels of PAHs in dust samples from the area of study did not pose significant health risk to population based on acute and intermediate oral exposure except for ACE. Accordingly, the correlation coefficients could be useful to identify possible sources of PAHs. The matrix of the PCC between the residue levels of individual PAHs in the examined 90 dust samples is presented in Table 9. Significant positive correlations at the 0.05 level were observed for the combinations of NAP/ACE = 0.405, FLR/ANT = 0.461, ANT/FLT = 0.431, FLT/IP = 0.363, PYR/BaP = 0.377, BaA/CHR = 0.402, CHR/BaP = 0.394 and BKF/IP = 0.382. In addition, significant positive correlations at the 0.01 level were observed for the combinations of FLR/BaA = 0.472, FLT/BKF = 0.479, PYR/BBF = 0.578, BaA/BaP = 0.469 and BaP/BghiP = 0.717. This result clearly indicates that PAHs are resulted from both pyrolytic and petrogenic origins. Significant levels at 0.01 level shows stronger association than that at 0.05 level.

Table 5: Factorial analysis for different recorded PAHs

Compound	Sector										Av	Min	Max
	I-IV	V-VIII	IX-XII	XIII-XVI	XVII-XVIII	XIX-XXI	XXII-XXIII	XXIV-XXV	XXVI-XXVII	XXVIII-XXX			
PHN/ANT	3.33	NR	2.41	2.32	NR	0.02	NR	0.23	0.21	NR	1.42	0.02	3.33
FLT/PYR	2.47	0.24	0.60	0.03	1.17	96.99	0.51	0.51	0.43	NR	11.44	0.03	96.99
BaA/CHR	0.21	229.94	0.64	0.31	0.87	NR	2.80	0.33	NR	NR	33.58	0.21	229.94
BaP/BghiP	1.39	1.44	2.38	2.35	1.26	NR	1.44	2.30	NR	NR	1.79	1.26	2.38
BbF/BaP	0.82	0.55	0.95	1.31	0.56	1.75	0.15	0.90	3.69	NR	1.19	0.15	3.69
BkF/BaP	0.11	0.85	0.66	NR	0.84	2.05	1.66	0.78	NR	NR	0.99	0.11	2.05
IP/BghiP	NR	2.09	21.06	3.39	5.78	NR	0.48	9.13	NR	NR	3.64	1.44	3.21
ANT/(ANT+PHE)	0.23	1.00	0.29	0.30	1.00	0.98	NR	0.81	0.83	NR	0.68	0.23	1.00
FLR/(FLR+PYR)	0.83	0.03	0.35	0.08	0.30	0.98	0.07	0.33	NR	NR	0.37	0.03	0.98
FLT/(FLT+PYR)	0.71	0.19	0.38	0.03	0.54	0.99	0.34	0.34	0.30	1.00	0.48	0.03	1.00
IP/(IP+BghiP)	NR	1.00	2.00	3.00	4.00	5.00	6.00	7.00	8.00	9.00	5.00	1.00	9.00
LMW PAHs	756.34	ND	3175.51	841.71	1242.13	732.82	2474.23	2233.55	2140.93	1121.41	1635.40	732.82	3175.51
HMW PAHs	494.07	808.74	1281.29	1591.39	2785.52	ND	1033.91	1385.13	1162.29	363.00	1211.70	363.00	2785.52
LWM/HMW	1.53	NR	2.48	0.53	0.45	NR	2.39	1.61	1.84	3.09	1.74	0.45	3.09
2-ring	68.24	672.46	240.84	169.65	46.20	31.48	215.58	246.87	35.81	15.44	174.26	15.44	672.46
3-rings	688.10	1210.84	2934.67	672.06	1195.94	701.34	2258.65	1986.67	2105.12	1105.96	1485.93	672.06	2934.67
4-rings	98.67	154.81	288.79	702.07	824.02	314.93	330.46	707.44	731.66	8.29	416.12	8.29	824.02
5-rings	373.83	500.91	390.75	606.77	624.44	348.20	607.68	274.34	430.63	NR	461.95	274.34	624.44
6-rings	21.57	153.02	601.75	282.55	1337.06	182.02	95.76	403.35	ND	354.71	381.31	21.57	1337.06

LMW PAHs = Low molecular weight of PAHs including two and three aromatic rings, HMW PAHs= high molecular weight PAHs compounds including four and six aromatic rings: 2-ring= NAP, 3-ring = ACY, ACE, FLU, PHE and ANT; 4- ring =FLT, PYR, BaA and CHR; 5-ring = BbF, BkF, BaP and DBA; 6-ring =BghiP and IP, ND = <DL, NR = not recorded because there is no value to be calculated.

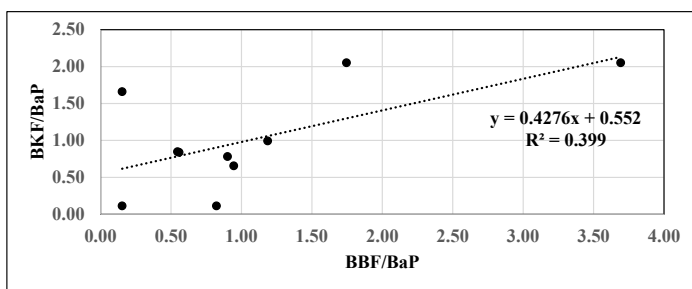


Figure 4: Relation between BbF/BaP with BkF/BaP

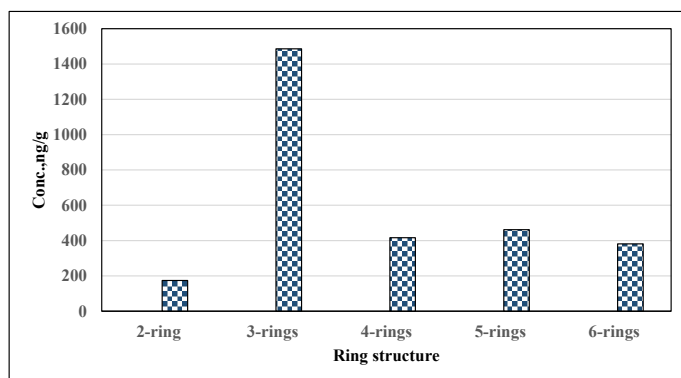


Figure 5: Distribution of concentrations (ng/g) of different ring structures of PAHs

Interestingly, no significant negative correlations were observed through the matrix; suggesting the absence of contradict sources of PAHs in the study area. The dendrogram obtained from the cluster analysis is depicted in Figure 6. As observed, the sampled sites could be classified into five cluster as follows: Cluster-A includes I, II, III, V, VII, XI, XIII, XIV, XIX, XXI and XXVI; Cluster-B includes IV, VIII, XV, XVI, XVII, XVIII, XX, XXIII, XXIV, XXV and XXVIII; Cluster-C includes VI, IX, X, XII, XXII and XXX; Cluster-D includes XXIX; Cluster-E includes XXVII.

Table 6: Hazardous quotients, hazardous indices, and cancer risks of potentially toxic PAHs in street dust for adults in the area of investigation

Compound	CD _{ingestion}	CD _{inhalation}	CD _{dermal}	RFD*	HQ			HI
					Ingestion	Inhalation	Dermal	
NAP	2.39E-04	3.51E-08	9.52E-07	0.02	1.19E-02	1.76E-06	4.76E-05	1.20E-02
ACY	2.91E-04	4.27E-08	1.16E-06	0.02	1.45E-02	2.14E-06	5.80E-05	1.46E-02
ACE	1.61E-03	2.37E-07	6.42E-06	0.06	2.68E-02	3.94E-06	1.07E-04	2.69E-02
FLR	8.04E-05	1.18E-08	3.21E-07	0.02	4.02E-03	5.91E-07	1.60E-05	4.04E-03
PHN	2.55E-05	3.75E-09	1.02E-07	0.04	6.37E-04	9.37E-08	2.54E-06	6.40E-04
ANT	2.96E-05	4.36E-09	1.18E-07	0.3	9.87E-05	1.45E-08	3.94E-07	9.91E-05
FLT	1.53E-04	2.25E-08	6.10E-07	0.04	3.82E-03	5.62E-07	1.53E-05	3.84E-03
PYR	2.61E-04	3.84E-08	1.04E-06	0.03	8.71E-03	1.28E-06	3.47E-05	8.74E-03
BaA	7.03E-05	1.03E-08	2.81E-07	NA	NR	NR	NR	NR
CHR	9.51E-05	1.40E-08	3.79E-07	NA	NR	NR	NR	NR
BBF	1.30E-04	1.92E-08	5.20E-07	NA	NR	NR	NR	NR
BKF	8.27E-05	1.22E-08	3.30E-07	NA	NR	NR	NR	NR
BaP	1.20E-04	1.76E-08	4.77E-07	NA	NR	NR	NR	NR
DBA	2.37E-04	3.48E-08	9.45E-07	NA	NR	NR	NR	NR
BghiP	1.25E-04	1.83E-08	4.98E-07	0.04	3.12E-03	4.58E-07	1.24E-05	3.13E-03
IP	3.58E-04	5.26E-08	1.43E-06	NA	NR	NR	NR	NR

Table 7: Hazardous quotients, hazardous indices, and cancer risks of potentially toxic PAHs in street dust for children in the area of investigation

Compound	CD _{ingestion}	CD _{inhalation}	CD _{dermal}	RFD	HQ			HI
					Ingestion	Inhalation	Dermal	
NAP	2.23E-03	6.23E-08	6.24E-07	0.02	1.11E-01	3.11E-06	3.12E-05	1.11E-01
ACY	2.71E-03	7.58E-08	7.59E-07	0.02	1.36E-01	3.79E-06	3.80E-05	1.36E-01
ACE	1.50E-02	4.20E-07	4.21E-06	0.06	2.50E-01	7.00E-06	7.01E-05	2.50E-01
FLR	7.51E-04	2.10E-08	2.10E-07	0.02	3.75E-02	1.05E-06	1.05E-05	3.75E-02
PHN	2.38E-04	6.65E-09	6.66E-08	0.04	5.95E-03	1.66E-07	1.66E-06	5.95E-03
ANT	2.76E-04	7.72E-09	7.74E-08	0.3	9.21E-04	2.57E-08	2.58E-07	9.22E-04
FLT	1.43E-03	3.99E-08	4.00E-07	0.04	3.57E-02	9.97E-07	9.99E-06	3.57E-02
PYR	2.44E-03	6.81E-08	6.82E-07	0.03	8.12E-02	2.27E-06	2.27E-05	8.13E-02
BaA	6.57E-04	1.83E-08	1.84E-07	NA	NR	NR	NR	NR
CHR	8.88E-04	2.48E-08	2.49E-07	NA	NR	NR	NR	NR
BBF	1.22E-03	3.40E-08	3.41E-07	NA	NR	NR	NR	NR
BKF	7.72E-04	2.16E-08	2.16E-07	NA	NR	NR	NR	NR
BaP	1.12E-03	3.12E-08	3.13E-07	NA	NR	NR	NR	NR
DBA	2.21E-03	6.17E-08	6.19E-07	NA	NR	NR	NR	NR
BghiP	1.16E-03	3.25E-08	3.26E-07	0.04	2.91E-02	8.13E-07	8.15E-06	2.91E-02
IP	3.34E-03	9.33E-08	9.35E-07	NA	NR	NR	NR	NR

Table 8: Factors used for calculation the LADDinh and CR

PAH	LADD		CR		DI ng/kg/day	MRLs, ng/kg/day
	Adults	Children	Adults	Children		
NAP	2.03E-07	8.113E-07	NR	NR	207.37	Acute 600, intermediate 600
ACY	6.172E-08	2.469E-07	NR	NR	252.38	
ACE	3.419E-07	1.368E-06	NR	NR	1398.14	intermediate 600
FLR	1.709E-08	6.835E-08	NR	NR	69.88	intermediate 400
PHE	5.413E-09	2.165E-08	NR	NR	22.14	
ANT	6.291E-09	2.516E-08	NR	NR	25.73	intermediate 10000
FLT	3.249E-08	1.299E-07	NR	NR	132.85	intermediate 400
PYR	5.548E-08	2.219E-07	NR	NR	226.87	NA
BaA	1.494E-08	5.977E-08	1.09E-08	4.36E-08	61.11	NA
CHR	2.02E-08	8.081E-08	1.41E-10	5.66E-10	82.62	NA
BBF	2.77E-08	1.108E-07	2.02E-08	8.09E-08	113.28	NA
BKF	1.758E-08	7.031E-08	1.28E-09	5.13E-09	71.88	NA
BaP	2.541E-08	1.016E-07	1.85E-07	7.42E-07	103.91	NA
DBA	5.029E-08	2.012E-07	3.67E-07	1.47E-06	205.67	NA
BghiP	2.649E-08	1.06E-07	NR	NR	108.32	NA
IP	7.603E-08	3.041E-07	5.55E-08	2.22E-07	310.90	NA

NA = not available, NR = not recorded as there is no value for CSF, MRLs =minimal risk levels, DI = daily intake, CR = carcinogenic risk, LADD = lifetime average daily dose.

Table 9: Pearson's correlation coefficient matrix of recorded PAHs in dust samples

PAH	NAP	ACY	ACE	FLR	PHE	ANT	FLT	PYR	BaA	CHR	BBF	BKF	BaP	DBA	BghiP	IP
NAP	1															
ACY	-0.148	1														
ACE	0.405*	-0.032	1													
FLR	-0.074	-0.060	0.154	1												
PHE	0.001	-0.048	0.042	-0.168	1											
ANT	-0.086	-0.152	-0.019	0.461*	-0.276	1										
FLT	-0.143	-0.257	-0.030	0.320	-0.206	0.431*	1									
PYR	0.060	-0.094	-0.204	-0.190	0.025	0.173	-0.195	1								
BaA	0.056	0.010	0.217	0.472**	0.073	0.302	0.088	-0.013	1							
CHR	-0.052	-0.007	0.058	0.097	0.054	0.289	-0.025	0.260	0.402*	1						
BbF	0.000	-0.129	-0.076	-0.066	0.087	0.250	0.266	0.578**	-0.035	-0.075	1					
BKF	0.352	-0.192	0.092	0.000	0.138	0.041	0.479**	-0.079	0.123	-0.160	0.279	1				
BaP	-0.017	-0.076	-0.141	0.193	-0.099	0.223	-0.087	0.377*	0.469**	0.394*	-0.014	-0.078	1			
DBA	0.010	-0.071	0.025	-0.030	0.145	0.068	0.115	0.032	0.183	-0.024	0.214	0.043	0.253	1		
BghiP	-0.129	-0.048	-0.132	-0.060	-0.070	0.096	0.016	0.317	0.348	0.342	0.143	0.208	0.717**	0.347	1	
IP	-0.080	-0.022	-0.070	0.112	0.005	0.236	0.363*	-0.004	0.175	0.205	0.286	0.382*	0.298	-0.167-	0.311	1

*Correlation is significant at the 0.05 level (2-tailed) ; **Correlation is significant at the 0.01 level (2-tailed).

The distribution could be related to the location of pollution sources. Cluster A: includes samples from Abha Industrial (I-III), Gold market area (V), Asdaf mole (VII), Khamees-Mushait industrial-2 (XI), Vegetables and Dates Market area (XIII), Abu Dabeel petrol station (XIV), Al-Beshri petrol station (XIX), Dana Olive Station (XXI), Al-Shuhada garden (XXVI). While Cluster B: includes samples from Lasan area (IV), Bahes Traffic light (VIII), Khamees-Mushait General Hospital (XV), Heef Concrete Factory (XVI), King Fahd Garden area (XVII), Al-Hayat National Hospital (XXIII), Khamees Avenue Mall area (XX), Al-Wajih Holding Company area (XXIII), Traffic light at Ahd Rofiadah (XXIV), Saif Muhammad Al Ddubsh area (XXV) and Dalagan Park area (XXVIII). The activities of clusters A and B: is classified as Industrial, traffic and commercial sources of pollution. The obtained dendrogram (Figure

6) Declared that the main source of pollution in both clusters is arranged in the following order Traffic > Industrial > Commercial. Nevertheless, Clusters D and E were nearer to each other than to Clusters A, B and C. To get more insight into the data structure, PCA was performed for concentrations of 16 EPA-PAHs as active variables and 30 sites. The total variance of PCA of the contents of 16-PAHs in dust samples collected from Khamees-Mushait city,

Saudi Arabia, is shown in **Table 10**. The initial Eigenvalues, in terms of the total variance, the % of the variance, and the cumulative % are all addressed as described [32, 33]. As observed, 7 components were considered principals, which represented 77.4% of the total variance and the eigenvalues of the extracted factors were > 1. The loadings of components were as follows: Component-1, Component-2, Component-3, Component-4, Component-5, Component-6 and Component-7: with 15.7%, 12.9%, 12.4%, 11.0%, 10.0%, 7.9%, 7.4%, respectively. The PCA distinguished five groups of PAHs. It could suggest that of both Component-2 and Component-3, besides Component-6 and Component-7, were loaded by almost similar content of PAHs. On the other hand, the rotated component matrix of PCA is shown in **Table 11**, while the plot of PCA: the first three principal components is shown in Figures (7-8). As observed, Component-1 was considerably loaded by BaA, CHR, BaP and BghiP with 0.562, 0.582, 0.894 and 0.851, respectively. While Component-2 was considerably loaded by FLR and ANT with 0.822 and 0.753, respectively. Additionally, whereas Component-3 was loaded by FLT, BkF and IP with 0.685, 0.856, and 0.698, respectively. Component-4 was loaded by PYR and BbF with 0.858 and 0.817, respectively.

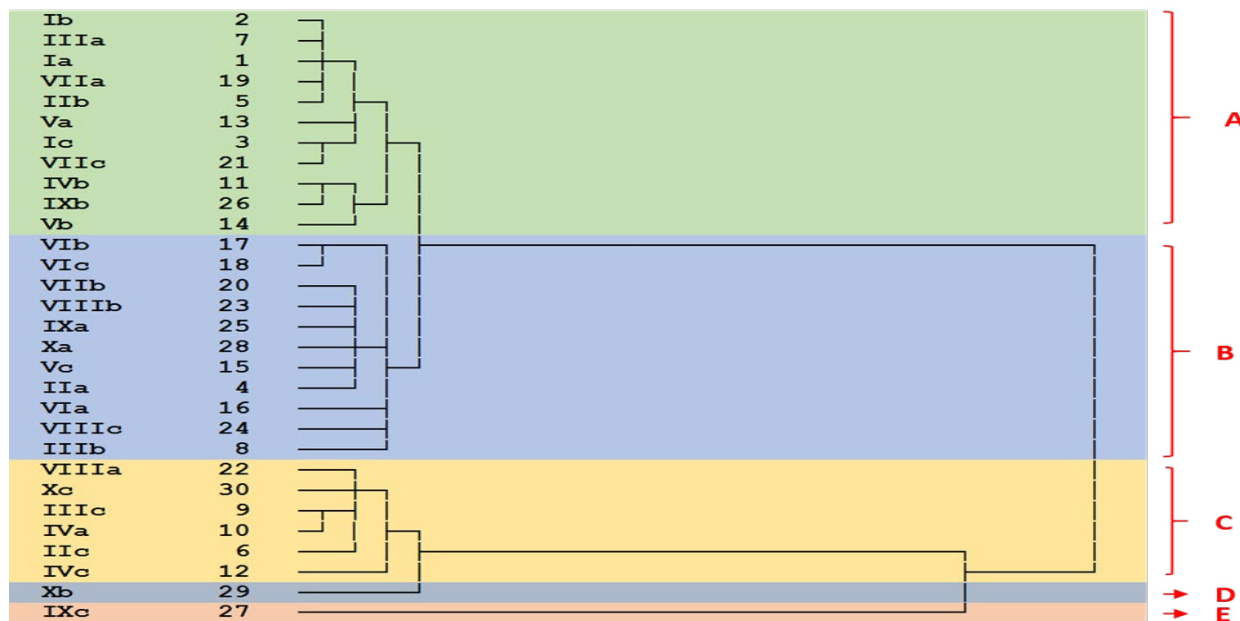


Figure 6: Dendrogram of the contents of five groups of PAHs (2-rings, 3-rings, 4-rings, 5-rings, and 6-rings).

Interestingly, the rest of components was loaded by one variable as follows: Component-5 NAP with 0.881, Component-6, DBA with 0.883, and Component-7 PHN with 0.911. PCA can reduce the number of variables and presented into main components. The first component in PCA represented 15.7 % of the total variance.

This component was highly loaded on medium, and HMW PAHs, which are mainly originated from fuel combustion and/or carcinogenic sources, and they are difficult to evaporate and degraded as mentioned by [34].

Table 10: Total variance of PCA of the contents of 16-PAHs in street dust samples collected from 30 sites in Khamees-Mushait city, Saudi Arabia

Component	Initial Eigenvalues			Extraction Sums of Squared Loadings			Rotation Sums of Squared Loadings		
	Total	% of Variance	Cumulative %	Total	% of Variance	Cumulative %	Total	% of Variance	Cumulative %
1	3.137	19.607	19.607	3.137	19.607	19.607	2.519	15.745	15.745
2	2.151	13.441	33.048	2.151	13.441	33.048	2.059	12.870	28.616
3	1.918	11.988	45.037	1.918	11.988	45.037	1.988	12.424	41.040
4	1.672	10.448	55.485	1.672	10.448	55.485	1.764	11.022	52.061
5	1.273	7.956	63.441	1.273	7.956	63.441	1.601	10.006	62.068
6	1.192	7.452	70.893	1.192	7.452	70.893	1.261	7.882	69.950
7	1.034	6.465	77.359	1.034	6.465	77.359	1.185	7.409	77.359
8	0.919	5.745	83.104						
9	0.690	4.312	87.416						
10	0.558	3.487	90.903						
11	0.446	2.787	93.690						
12	0.322	2.013	95.703						
13	0.308	1.922	97.625						
14	0.217	1.355	98.980						
15	0.098	0.612	99.592						
16	0.065	0.408	100.000						

Table 11: Rotated component matrix of principal component analysis of the contents of 16-PAHs in street dust samples collected from 30 sites in Abha and Khamees-Mushait city, Saudi Arabia

PAH	Component						
	1	2	3	4	5	6	7
NAP	0.003	-0.183	0.093	0.094	0.881	-0.007	-0.105
ACY	0.055	-0.129	-0.207	-0.301	-0.249	-0.271	0.163
ACE	-0.078	0.221	-0.035	-0.169	0.733	0.000	0.175
FLR	0.049	0.822	0.040	-0.187	0.052	0.011	-0.069
PHN	-0.053	-0.168	0.035	0.064	0.029	0.095	0.911
ANT	0.119	0.753	0.107	0.340	-0.071	-0.020	-0.230
FLT	-0.174	0.478	0.685	0.053	-0.161	0.179	-0.186
PYR	0.330	-0.124	-0.210	0.858	-0.012	-0.077	-0.020
BaA	0.562	0.540	0.049	-0.164	0.216	0.082	0.270
CHR	0.582	0.322	-0.174	0.130	0.032	-0.328	0.212
BbF	-0.064	0.054	0.322	0.817	-0.082	0.137	0.138
BkF	0.010	-0.088	0.856	0.055	0.298	0.097	0.077
BaP	0.894	0.103	-0.039	0.088	-0.045	0.100	-0.137
DBA	0.232	0.034	-0.014	0.069	-0.028	0.883	0.149
BghiP	0.851	-0.123	0.220	0.096	-0.133	0.228	-0.071
IP	0.340	0.120	0.698	0.074	-0.164	-0.394	0.077

It can be noticed that BghiP and CHR are presented in these components, which are evidence that these chemical compounds are originated from petroleum burning. It is suggesting that the prima-

ry component emissions from traffic sources, as it is well known that IP, BghiP, BaP, FLT, and PYR are markers for vehicle emissions as declared by [35].

Table 12 : A Comparison between PAH Concentrations of the Present Study With Other Area of the Surroundings

Location	Type of sample	MIN	MAX	AV	Reference
Khamees- Mushait, KSA	outdoor	1250.41	4249.29	2809.46	Present study
Jeddah, KSA	Indoor	950	11950	3750	Ali et al., 2016
	Indoor	1150	14500	4800	
	outdoor	480	8050	2750	
	outdoor	7620	30800	14200	Ali et al., 2017
Riyadh, KSA	Outdoor	90	22146	4096	El-Mubarak et al., 2016
Doha, Qatar	Indoor	1.6	477.3	206	Mahfouz et al., 2019
Jordan, Amman	Outdoor	13240	499600	--	Jiries 2003
Egypt	Outdoor	27	379	130.5	Mostafa et al., 2009
Bushehr, Iran	Outdoor	73.6	9491	1116.02	Keshavarzi et al., 2020
Karaj, northern Iran	Outdoor	16.2	1236.2	624	Qishlaqi and Beirama-li 2019
Kocaeli, Turkey	Indoor	85.91	40359	5680	Civan and Kara 2016
Asansol, India	Outdoor	1708	9688	4532	Gope et al., 2018
Guwahati, India	Outdoor, during moon soon	2248.8	13550	8500.8	Hussain et al. 2015
	Outdoor, during post-moon soon	1394.7	43789	23294.7	
	Outdoor, during pre-moon soon	5153.5	28796.3	14770.5	
Hunan, China	Outdoor	3515	24488	8760	Long et al., 2011
Gungzhou, South China	Outdoor	840	12300	4800	Wang et al., 2011
Northwest China	Outdoor	1240	10700	3900	Jang et al., 2014
Xuzhou, China	Outdoor	2174	24499	6616	Wang et al., 2017
Hanggang, Central China	Outdoor	622.97	4340.67	1862.10	Liu et al., 2019
Chengdu, China	Outdoor	2.15	10.6	4.61	Li et al., 2021
Sydney, Australia	Outdoor	9000	105000	--	Aryal et al., 2011
Niger Delta, Nigeria	Outdoor	165. 1	1012	--	Iwegbue and Obi 2016
Novi Sad, Serbia	Outdoor (summer)	35	2422	638	Skrbic et al., 2019
	Outdoor (winter)	35	587	221	

In addition, changing engine oil along roadsides along with fuel filling for vehicles is seen regularly every day in khamees-mushait, which is the major cause of oil spillage. Table 12 shown concentrations of PAHs recorded in street dust in the area of investigation with that in different areas of the surroundings. The degree

of dust contamination by PAHs in current study was lower than that recorded in Jeddah and Riyad (KSA). In addition, these values were comparable to Arabian Gulf area and lower than that of Asian countries.

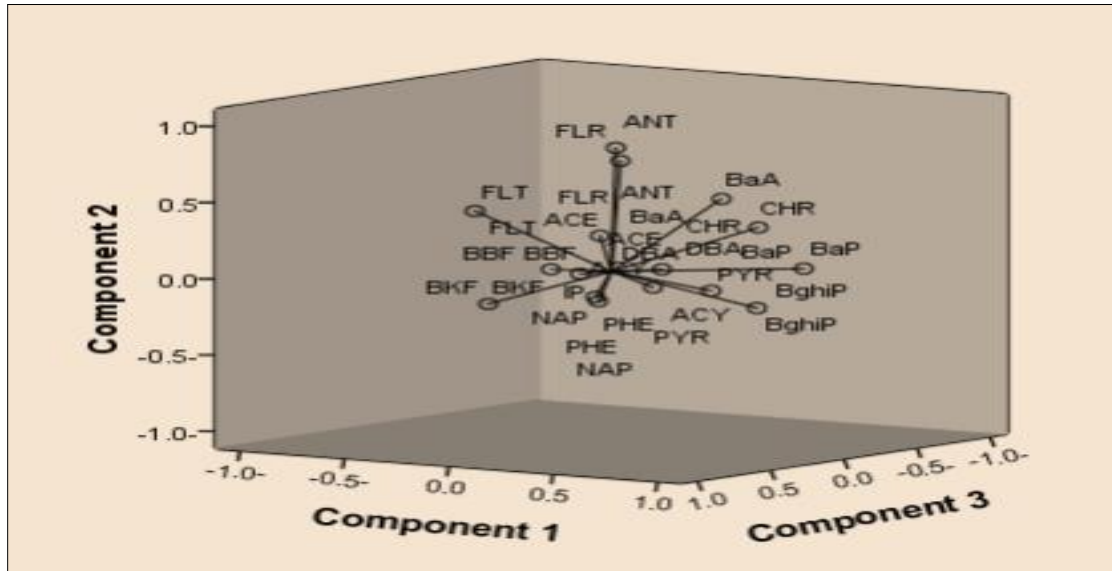


Figure 7: Principal component analysis plot of the contents of 16-PAHs in dust samples collected from 30 sites in Khamees-Mushait city, Saudi Arabia

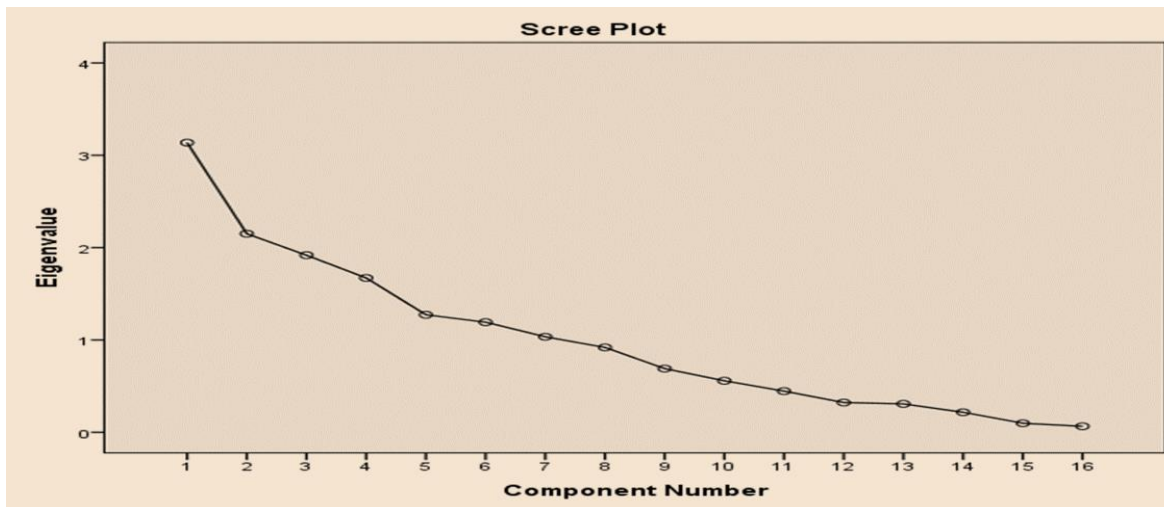


Figure 8: Eigen values plot of the contents of 16-PAHs in dust samples collected from 30 sites in Khamees-Mushait city, Saudi Arabia

Conclusion

Various approaches (geochemical indices, statistical analysis, and health risk assessment) were exploited to evaluate the levels of 16-PAHs in street dust from Abha and Khamees-Mushait city, Saudi Arabia. It was obvious that the decreasing order of average PAHs categories was Σ FPAHs > Σ CARC > Σ COMB for all sectors. All locations had concentrations much higher than of the ERL, ERM, TEL and PEL levels. The diagnostic ratios suggest that PAHs in the street dust originated from the pyrolytic and petrogenic processes, especially the incomplete combustion of organic materials. The HQ, HI non-cancerous, and cancers risk values of PAHs for adults and children were < 1. This result suggests safe levels of the quantified PAHs in all dust sample [36-53]. The carcinogen

risks from inhalation exposure pathway for adults and children of all PAHs were generally within the acceptable risk level (1×10^{-6}). The residual levels of PAHs in dust samples from the area of study did not pose significant health risk to population based on acute and intermediate oral exposure except for ACE.

Author Contributions Idea and Protocol Design

Tarek O. Said, Nasser S. Awwad and Fatimah A. Alamri

Methodology and Experimentation

Tarek O. Said, Fatimah A. Alamri, Nasser S. Awwad and Ali Y. Alamie.

Data Analysis

Tarek O. Said, Fatimah A. Alamri, Nasser S. Awwad and Abubakr M. Idris.

All Authors Shared Draft Writing

All authors approved the submission

Funding

The authors have no relevant financial or non-financial interests to disclose.

Data Availability Statement

All required data will be available with the corresponding author upon request.

Conflict of Interest Statement

The authors declare that they have no conflict of interest.

Consent for Publication

All authors approve this submission.

Consent to Participate

Not applicable as the study did not include human subject.

Compliance with Ethical Standards

The present manuscript is not submitted to more than one journal for simultaneous consideration. The submitted work is original and have not been published elsewhere in any form or language (partially or in full). The results are presented clearly, honestly, and without fabrication, falsification, or inappropriate data manipulation. Authors adhere to discipline-specific rules for acquiring, selecting, and processing data. All authors agreed with the content and that, all gave explicit consent to submit and that they obtained consent from the responsible authorities at the institute/organization where the work has been carried out before the work is submitted. Authors are responsible for correctness of the statements provided in the manuscript. All authors certify that they have no affiliations with or involvement in any organization or entity with any financial interest or non-financial interest in the subject matter or materials discussed in this manuscript

References

1. Liu, J., Zhang, J., Zhan, C., Liu, H., Zhang, L., Hu, T., & Qu, C. (2019). Polycyclic aromatic hydrocarbons (PAHs) in urban street dust of Huanggang, central China: Status, sources and human health risk assessment. *Aerosol and Air Quality Research*, 19(2), 221-223.
2. Xu, L., Shu, X., & Hollert, H. (2017). Aggregate risk assessment of polycyclic aromatic hydrocarbons from dust in an urban human settlement environment. *Journal of Cleaner Production*, 133, 378-388.
3. Ma, Y., Liu, A., Egodawatta, P., McGree, J., & Goonetilleke, A. (2017). Quantitative assessment of human health risk posed by polycyclic aromatic hydrocarbons in urban road dust. *Science of the Total Environment*, 575, 895-904.
4. USEPA. (1984). Guidelines establishing test procedures for the analysis of pollutants under clean water act: method 610 – Polynuclear aromatic hydrocarbons. *Federal Register*, 49, 43344–43352.
5. Wei, Y., Han, I. K., Hu, M., Shao, M., Zhang, J. J., & Tang, X. (2010). Personal exposure to particulate PAHs and anthraquinone and oxidative DNA damages in humans. *Chemosphere*, 81(10), 1280-1285.
6. Wang, X. S. (2018). Polycyclic aromatic hydrocarbons in urban street dust: sources and health risk assessment. *Environmental geochemistry and health*, 40(1), 383-393.
7. Bi, C., Chen, Y., Zhao, Z., Li, Q., Zhou, Q., Ye, Z., & Ge, X. (2020). Characteristics, sources and health risks of toxic species (PCDD/Fs, PAHs and heavy metals) in PM_{2.5} during fall and winter in an industrial area. *Chemosphere*, 238, 124620.
8. Singh, L., Varshney, J. G., & Agarwal, T. (2016). Polycyclic aromatic hydrocarbons' formation and occurrence in processed food. *Food Chemistry*, 199, 768-781.
9. Alghamdi, M. A., Alam, M. S., Yin, J., Stark, C., Jang, E., Harrison, R. M., & Shabbaj, I. I. (2015). Receptor modelling study of polycyclic aromatic hydrocarbons in Jeddah, Saudi Arabia. *Science of the Total Environment*, 506, 401-408.
10. Alghamdi, M. A., Hassan, S. K., Alzahrani, N. A., Al Sharif, M. Y., & Khoder, M. I. (2020). Classroom dust-bound polycyclic aromatic hydrocarbons in Jeddah primary schools, Saudi Arabia: level, characteristics and health risk assessment. *International journal of environmental research and public health*, 17(8), 2779.
11. El-Mubarak, A. H., Rushdi, A. I., Al-Mutlaq, K. F., Al Mdaawi, F. Z., Al-Hazmi, K., Dumenden, R. S., & Pascua, R. A. (2016). Polycyclic aromatic hydrocarbons and trace metals in mosque's carpet dust of Riyadh, Saudi Arabia, and their health risk implications. *Environmental Science and Pollution Research*, 23(21), 21273-21287.
12. Li, H. H., Yang, Z. B., Xu, X. X., Zhu, X. M., Xian, J. R., Yang, Y. X., & Cheng, Z. (2022). Polycyclic aromatic hydrocarbons in street dust from different functional areas in Chengdu, China: seasonal variation and health risk assessment. *Environmental geochemistry and health*, 44(3), 1161-1173.
13. Idris, A. M., Alqahtani, F. M., Said, T. O., & Fawy, K. F. (2018). Contamination level and risk assessment of heavy metal deposited in street dusts in Khamees-Mushait city, Saudi Arabia. *Human and ecological risk assessment: an international journal*, 26(2), 495-511.
14. Idris, A. M., Said, T. O., Brima, E. I., Sahlabji, T., Alghamdi, M. M., El-Zahhar, A. A., & El Nemr, A. M. (2019). Assessment of contents of selected heavy metals in street dust from Khamees-Mushait city, Saudi Arabia using multivariate statistical analysis, GIS mapping, geochemical indices and health risk. *Fresen Environ Bull*, 28(8), 6059-69.
15. USEPA (2002). Supplemental guidance for developing soil screening levels for superfund sites. Environmental Protection Agency, Washington, DC.

16. United States Department of Energy. (2011). The Risk Assessment Information System (RAIS). U.S. Department of Energy's Oak Ridge Operations Office, Washington, DC.
17. USEPA. (1996). Method 3050B: Acid Digestion of Sediments, Sludges, and Soils, Revision 2., 12pp.
18. USEPA. (2001a). Integrated Risk Information System (IRIS). National Center for Environmental Assessment. Office of Science and Technology, Washington, DC.
19. USEPA. (2001b). Supplemental guidance for developing soil screening levels for superfund sites. Guidance for Dermal Risk Assessment. Interim Guidance, OSWER 9355.
20. ATSDR, T. (2018). ATSDR (Agency for toxic substances and disease registry). Prepared by clement international corp., under contract, 205, 88-0608.
21. CCME. (2001). Canadian sediment quality guidelines for the protection of aquatic life, Toronto, Canada, 26pp.
22. Latimer, J. S., Hoffman, E. J., Hoffman, G., Fasching, J. L., & Quinn, J. G. (1990). Sources of petroleum hydrocarbons in urban runoff. *Water, Air, and Soil Pollution*, 52(1), 1-21.
23. Long, E. R., MacDonald, D. D., Smith, S. L., & Calder, F. D. (1995). Incidence of adverse biological effects within ranges of chemical concentrations in marine and estuarine sediments. *Environmental management*, 19(1), 81-97.
24. Yunker, M. B., Macdonald, R. W., Vingarzan, R., Mitchell, R. H., Goyette, D., & Sylvestre, S. (2002). PAHs in the Fraser River basin: a critical appraisal of PAH ratios as indicators of PAH source and composition. *Organic geochemistry*, 33(4), 489-515.
25. Zhang, Y., Dou, H., Chang, B., Wei, Z., Qiu, W., Liu, S., & Tao, S. (2008). Emission of polycyclic aromatic hydrocarbons from indoor straw burning and emission inventory updating in China. *Annals of the New York Academy of Sciences*, 1140(1), 218-227.
26. Tobiszewski, M., & Namieśnik, J. (2012). PAH diagnostic ratios for the identification of pollution emission sources. *Environmental pollution*, 162, 110-119.
27. Baumard, P., Budzinski, H., Michon, Q., Garrigues, P., Burgeot, T., & Bellocq, J. (1998). Origin and bioavailability of PAHs in the Mediterranean Sea from mussel and sediment records. *Estuarine, Coastal and Shelf Science*, 47(1), 77-90.
28. Sicre, M. A., Marty, J. C., Saliot, A., Aparicio, X., Grimalt, J., & Albaiges, J. (1987). Aliphatic and aromatic hydrocarbons in different sized aerosols over the Mediterranean Sea: occurrence and origin. *Atmospheric Environment* (1967), 21(10), 2247-2259.
29. Mandalakis, M., Tsapakis, M., Tsoga, A., & Stephanou, E. G. (2002). Gas-particle concentrations and distribution of aliphatic hydrocarbons, PAHs, PCBs and PCDD/Fs in the atmosphere of Athens (Greece). *Atmospheric environment*, 36(25), 4023-4035.
30. Budzinski, H., Jones, I., Bellocq, J., Pierard, C., & Garrigues, P. H. (1997). Evaluation of sediment contamination by polycyclic aromatic hydrocarbons in the Gironde estuary. *Marine chemistry*, 58(1-2), 85-97.
31. Mostert, M. M., Ayoko, G. A., & Kokot, S. (2010). Application of chemometrics to analysis of soil pollutants. *TrAC Trends in Analytical Chemistry*, 29(5), 430-445.
32. Shen, M., Liu, G., Yin, H., & Zhou, L. (2020). Distribution, sources and health risk of PAHs in urban air-conditioning dust from Hefei, East China. *Ecotoxicology and Environmental Safety*, 194, 110442.
33. Grmasha, R. A., Al-sareji, O. J., Salman, J. M., & Hashim, K. S. (2020). Polycyclic aromatic hydrocarbons (PAHs) in urban street dust within three land-uses of Babylon governorate, Iraq: Distribution, sources, and health risk assessment. *Journal of King Saud University-Engineering Sciences*.
34. Liu, B., Xue, Z., Zhu, X., & Jia, C. (2017). Long-term trends (1990-2014), health risks, and sources of atmospheric polycyclic aromatic hydrocarbons (PAHs) in the US. *Environmental pollution*, 220, 1171-1179.
35. Keshavarzi, B., Abbasi, S., Moore, F., Mehravar, S., So-rooshian, A., Soltani, N., & Najmeddin, A. (2018). Contamination level, source identification and risk assessment of potentially toxic elements (PTEs) and polycyclic aromatic hydrocarbons (PAHs) in street dust of an important commercial center in Iran. *Environmental management*, 62(4), 803-818.
36. Ali, N., Ismail, I. M. I., Khoder, M., Shamy, M., Alghamdi, M., Costa, M., & Eqani, S. A. M. A. S. (2016). Polycyclic aromatic hydrocarbons (PAHs) in indoor dust samples from Cities of Jeddah and Kuwait: Levels, sources and non-dietary human exposure. *Science of the total environment*, 573, 1607-1614.
37. Ali, N., Ismail, I. M. I., Khoder, M., Shamy, M., Alghamdi, M., Al Khalaf, A., & Costa, M. (2017). Polycyclic aromatic hydrocarbons (PAHs) in the settled dust of automobile workshops, health and carcinogenic risk evaluation. *Science of the Total Environment*, 601, 478-484.
38. Aryal, R., Baral, B., Vigneswaran, S., Naidu, R., & Loganathan, P. (2011). Seasonal influence on urban dust PAH profile and toxicity in Sydney, Australia. *Water Science and Technology*, 63(10), 2238-2243.
39. Civan, M. Y., & Kara, U. M. (2016). Risk assessment of PBDEs and PAHs in house dust in Kocaeli, Turkey: levels and sources. *Environmental Science and Pollution Research*, 23(23), 23369-23384.
40. Gope, M., Masto, R. E., George, J., & Balachandran, S. (2018). Exposure and cancer risk assessment of polycyclic aromatic hydrocarbons (PAHs) in the street dust of Asansol city, India. *Sustainable cities and society*, 38, 616-626.
41. Hussain, K., Rahman, M., Prakash, A., & Hoque, R. R. (2015). Street dust bound PAHs, carbon and heavy metals in Guwahati city-Seasonality, toxicity and sources. *Sustainable Cities and Society*, 19, 17-25.
42. Idris, A. M., Alqahtani, F. M., Said, T. O., & Fawy, K. F. (2020). Contamination level and risk assessment of heavy metal deposited in street dusts in Khamees-Mushait city, Saudi Arabia. *Human and ecological risk assessment: an international journal*, 26(2), 495-511.
43. Idris, A. M., Said, T. O., Brima, E. I., Sahlabji, T., Alghamdi,

- M. M., El-Zahhar, A. A., & El Nemr, A. M. (2019). Assessment of contents of selected heavy metals in street dust from Khamees-Mushait city, Saudi Arabia using multivariate statistical analysis, GIS mapping, geochemical indices and health risk. *Fresen Environ Bull*, 28(8), 6059-69.
44. Iwegbue, C. M., & Obi, G. (2016). Distribution, sources, and health risk assessment of polycyclic aromatic hydrocarbons in dust from urban environment in the Niger Delta, Nigeria. *Human and Ecological Risk Assessment: An International Journal*, 22(3), 623-638.
45. Jiang, Y., Hu, X., Yves, U. J., Zhan, H., & Wu, Y. (2014). Status, source and health risk assessment of polycyclic aromatic hydrocarbons in street dust of an industrial city, NW China. *Ecotoxicology and environmental safety*, 106, 11-18.
46. Jiries, A. (2003). Vehicular contamination of dust in Amman, Jordan. *Environmentalist*, 23(3), 205-210.
47. Keshavarzi, B., Abbasi, S., Moore, F., Delshab, H., & Soltani, N. (2017). Polycyclic aromatic hydrocarbons in street dust of Bushehr City, Iran: status, source, and human health risk assessment. *Polycyclic Aromatic Compounds*.
48. Long, Y., Chi, G., Qing, H., Dai, T., & Wu, Q. (2011). Sources of polycyclic aromatic hydrocarbons in street dust from the Chang-Zhu-Tan Region, Hunan, China. *Journal of Environmental Protection*, 2(10), 1331.
49. Mahfouz, M. M., Hassan, H. M., Elobaid, E. A., Yigiterhan, O., & Alfoldy, B. (2019). PAH concentrations and exposure assessment from house dust retained in air-conditioning filters collected from Greater Doha, Qatar. *Environmental geochemistry and health*, 41(5), 2251-2263.
50. Mostafa, A. R., Hegazi, A. H., El-Gayar, M. S., & Andersson, J. T. (2009). Source characterization and the environmental impact of urban street dusts from Egypt based on hydrocarbon distributions. *Fuel*, 88(1), 95-104.
51. Qishlaqi, A., & Beiramali, F. (2019). Potential sources and health risk assessment of polycyclic aromatic hydrocarbons in street dusts of Karaj urban area, northern Iran. *Journal of Environmental Health Science and Engineering*, 17(2), 1029-1044.
52. Wang, W., Huang, M. J., Kang, Y., Wang, H. S., Leung, A. O., Cheung, K. C., & Wong, M. H. (2011). Polycyclic aromatic hydrocarbons (PAHs) in urban surface dust of Guangzhou, China: status, sources and human health risk assessment. *Science of the total environment*, 409(21), 4519-4527.
53. Wang, X. S., Chen, M. Q., & Zheng, X. (2017). Polycyclic aromatic hydrocarbons (PAHs) in Xuzhou urban street dust: concentration and sources. *Environmental Earth Sciences*, 76(16), 1-8.

Copyright: ©2022 Tarek O. Said, et al. This is an open-access article distributed under the terms of the Creative Commons Attribution License, which permits unrestricted use, distribution, and reproduction in any medium, provided the original author and source are credited.